Uncertainty and correlation analysis of lead nuclear data on reactor parameters for the European Lead Cooled Training Reactor

E. Alhassan[a], H. Sjöstrand[a], P. Helgesson[a], A. J. Koning[a,b], M. Österlund[a], S. Pomp[a], D. Rochman[b]

[a]*Division of Applied Nuclear Physics, Department of Physics and Astronomy, Uppsala University, Uppsala, Sweden*
[b]*Nuclear Research and Consultancy Group (NRG), Petten, The Netherlands*

Abstract

The Total Monte Carlo (TMC) method was used in this study to assess the impact of ^{204,206,207,208}Pb nuclear data uncertainties on reactor safety parameters for the ELECTRA reactor. Relatively large uncertainties were observed in the k_{eff} and the coolant void worth (CVW) for all isotopes except for ^{204}Pb with significant contribution coming from ^{208}Pb nuclear data; the dominant effect came from uncertainties in the resonance parameters; however, elastic scattering cross section and the angular distributions also had significant impact. It was also observed that the k_{eff} distribution for ^{206,207,208}Pb deviates from a Gaussian distribution with tails in the high k_{eff} region. An uncertainty of 0.9% on the k_{eff} and 3.3% for the CVW due to lead nuclear data were obtained. As part of the work, cross section-reactor parameter correlations were also studied using a Monte Carlo sensitivity method. Strong correlations were observed between the k_{eff} and (n, el) cross section for all the lead isotopes. The correlation between the (n, inl) and the k_{eff} was also found to be significant.

Keywords: TMC, nuclear data uncertainty, lead isotopes, safety parameters, ELECTRA, fuel cycle

Email addresses: erwin.alhassan@physics.uu.se (E. Alhassan), henrik.sjostrand@physics.uu.se (H. Sjöstrand)

1. Introduction

Evaluated nuclear data are required for computations and experimental support for a variety of applications ranging from nuclear reactor physics, nuclear criticality safety, medical physics, radiation protection [1], to national security and dosimetry. These data include information on nuclear reactions, decay data and fission yields, etc., which are important for the development of nuclear reaction models and are used in neutron transport codes for reactor core calculations [2]. All neutronic reactor parameters computed with modern transport codes are affected by the uncertainties in the underlying nuclear data used. To quantify the impact of these uncertainties on reactor parameters, nuclear data covariance information which come with modern nuclear data libraries are often used. These covariance data which contains the relative variances and covariances, relies on the assumption of normal distributions and are usually not complete [3, 4]. Furthermore, they are complicated to use. A consequence being that, the output of neutron transport codes are usually not accompanied by uncertainties due to nuclear data. However, quantifying and understanding these uncertainties is important for designing Generation IV (GEN-IV) reactors and for the optimization of current reactor technology [5]. The present work focuses on the propagation of nuclear data on reactor safety parameters using the SERPENT Monte Carlo code.

Until recently, nuclear data uncertainties within the reactor physics community were mostly propagated using perturbation methods which combine the sensitivity profile and covariance data to obtain the final uncertainties on reactor parameters [6]. For instance, the sensitivity profile can be obtained by using the so-called perturbation card in MCNP [7]. A new method for nuclear data uncertainty propagation - the Total Monte Carlo (TMC) method, was developed around the TALYS code [8] which incorporates microscopic nuclear physics and macroscopic nuclear reactor design into one simulation scheme [9]. The TMC approach has the capability of quantifying the impact of nuclear data uncertainties on reactor parameters directly from nuclear reaction model parameters.

This has an added advantage since a sensitivity feedback can be given to both experimental and model calculations for determining where additional efforts could be undertaken to reduce nuclear data uncertainties. The methodology has been tested extensively on a large number of criticality-safety, fusion and shielding benchmarks [10]. It was observed from the study that the usual assumption of Gaussian shape used by the perturbation approach for cross section uncertainty distributions was not always true and therefore should be taken into account in the development of future nuclear energy systems.

The Lead Fast Reactor (LFR) was selected by the Generation IV International Forum (GIF) as one of the six most promising advanced reactor concepts and was ranked top in sustainability because it uses a closed fuel cycle for the conversion of fertile isotopes, and in proliferation resistance and physical protection due to its long-life core [11]. Its safety features are enhanced by the choice of a relatively inert coolant which has the capability of retaining hazardous radionuclides such as iodine and cesium even in the event of a severe accident. As part of GEN-IV development in Sweden, the GENIUS project which is a collaboration between Royal Institute of Technology (KTH), Chalmers and Uppsala University was initiated for the enhancement and development of the technology relevant to the GEN-IV development [12]. The development of a lead-cooled Fast Reactor called ELECTRA - European Lead-Cooled Training Reactor which will permit full recycling of plutonium and americium in the core was proposed within this project. The isotopic abundance of lead is made up of 1.4% ^{204}Pb, 24.1% ^{206}Pb, 22.1% ^{207}Pb and 52.4% of ^{208}Pb. In Table 1, we compare results obtained by varying lead nuclear data from other nuclear data libraries using the SERPENT Monte Carlo code [13]. The data of all other isotopes were maintained as JEFF-3.1 [14] while the nuclear data for each lead isotope obtained from the following data libraries: ENDF/B-VII.1 [15], JENDL-4.0 [16], TENDL-2014 beta [17] and TENDL-2012 [18] were varied one after the other. A mean k_{eff} of 0.99877 with an average statistical uncertainty of 34 pcm was obtained for ^{208}Pb with a corresponding standard deviation of 340 pcm among the five libraries studied. From the relatively large spread observed between

Table 1: Comparison of k_{eff} results due to variation of lead nuclear data from other nuclear data libraries. All other isotopes except the isotope investigated were maintained as JEFF-3.1. The average statistical uncertainty obtained is 34 pcm.

	Nuclear data libraries				
k_{eff}	JEFF-3.1	ENDF/B-VII.1	JENDL-4.0	TENDL-2014 beta	TENDL-2012
^{208}Pb	1.00307	0.99642	1.00111	0.99626	1.00732
^{207}Pb	1.00307	1.00261	1.00233	1.00459	1.00212
^{206}Pb	1.00307	1.00212	1.00309	1.00107	1.01073
^{204}Pb	1.00307	1.00235	1.00274	1.00186	1.00224

the major nuclear data libraries, we can draw the conclusion that, the current ^{208}Pb nuclear data can be improved and therefore quantifying its uncertainty on reactor safety parameters is highly relevant for current and future nuclear reactor systems.

ELECTRA is cooled by pure lead and therefore nuclear data uncertainties of lead isotopes are expected to impact significantly the core and fuel cycle of the reactor. In this work, the TMC methodology was applied to ELECTRA to study the impact of ^{204,206,207,208}Pb nuclear data uncertainties on macroscopic parameters. These parameters include the effective multiplication factor, coolant temperature coefficient, coolant void worth and the effective delayed neutron fraction.

1.1. Total Monte Carlo

The TMC methodology used in this paper was first proposed by Koning and Rochman in 2008 [9] for nuclear data uncertainty propagation. In this method, theoretical nuclear model parameters are varied all together within pre-determined ranges derived from comparison with experimental cross section data to create TALYS inputs [19]. To create a complete ENDF file covering from thermal to fast neutron energies, non-Talys data such as the neutron resonance data, total (n,tot), elastic (n,el), capture (n,γ) or fission (n,f) cross sections at low neutron energies, average number of fission neutrons, and fission neutron spectra are added to results obtained from the TALYS code using other auxiliary codes [19] such as, the TARES code [20] for resonance parameters. In this way, nuclear reactions from thermal energy up to 20 MeV are covered [10]. A large set of random nuclear data can now be produced and then processed into

ENDF format using the TEFAL code [21]. For use in Monte Carlo codes such as SERPENT [22] or MCNP [7], the ACER module in NJOY [23] is used to convert the random ENDF nuclear data files into ACE files. In Fig. 1, we plot the (n,el) and (n,γ) of 50 random ACE ^{208}Pb files as a function of incident neutron energy. A spread in data can be observed for the entire energy region as presented in Fig. 1. This is expected as each file contains a unique set of nuclear data.

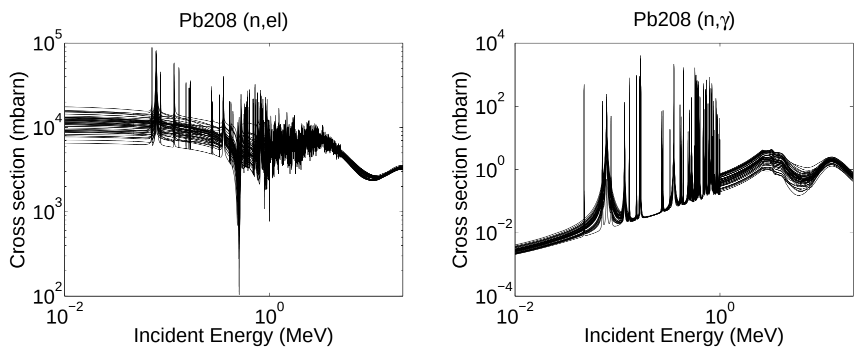

Figure 1: 50 random ACE ^{208}Pb cross sections plotted as a function of incident neutron energy. Left: ^{208}Pb(n,el) and right: ^{208}Pb(n,γ). Note that each random ACE files contain a unique set of nuclear data.

Depending on the variation of the nuclear data, different distributions with their corresponding mean values and standard deviations can be obtained for different quantities such as k_{eff}, fuel inventory, temperature feedback coefficients, kinetic parameters etc. [24]. By varying nuclear data within ranges predetermined by comparison to uncertainties in experimental measurements using the TMC methodology, the total variance of a physical observable (σ^2_{obs}) in the case of Monte Carlo codes can be expressed as:

$$\sigma^2_{obs} = \sigma^2_{ND} + \overline{\sigma^2_{stat}} \tag{1}$$

where σ^2_{ND} is the variance of the physical observable or parameter under study due to nuclear data uncertainties and, σ^2_{stat} is the variance due to statistics from the Monte Carlo code. With this approach called "original TMC", the time for a single calculation is increased by a factor of n where n (the number of samples or random files) ≥ 500 making it not suitable for some applications. As a solution, a faster method called the "Fast TMC" was developed [25]. By changing the seed of the random number generator within the Monte Carlo code and changing nuclear data at the same time, a spread in the data that is due to both statistics and nuclear data is obtained. By using different seeds for a large set of nuclear data, a more accurate estimate of the spread due to statistics is obtained and therefore the statistical requirement on each run could be lowered, thereby reducing the computational time involved for each calculation. A detailed presentation of fast TMC methodology is found in Ref. [25, 26, 27]. Fast TMC is the method used in this work. In Fig. 2, we present a summary of the TMC method in a flow chart. From the diagram, model parameters in the

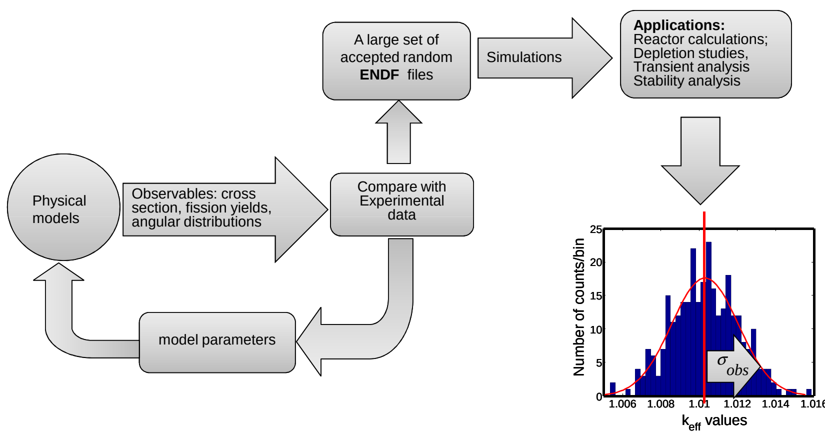

Figure 2: A flowchart depicting the Total Monte Carlo approach for nuclear data uncertainty analysis. Random files generated using the TALYS based, T6 code package [19] are processed and used to propagate nuclear data uncertainties in reactor calculations.

TALYS based code system called T6 [19] are adjusted after comparing physical observables such as cross sections, angular distributions, etc, with differential experimental data and a large set of random files are accepted. These random files are processed and used for simulations in reactor core calculations to obtain the reactor parameters and their uncertainties due to nuclear data.

1.2. Reactor Description

The ELECTRA - European Lead-Cooled Training Reactor is a conceptual 0.5 MW lead cooled reactor fueled with (Pu,Zr)N [12]. The fuel composition is made up of 60% mol of ZrN and 40% mol of PuN. The core is hexagonally shaped and it is 100% cooled by natural convection. The control assemblies and the absorbent part of control drums are made of B_4C. Fig. 3 shows the radial configurations of the ELECTRA core with control rods fully inserted. It is envisaged that ELECTRA will provide practical experience and data for research related to the development of GEN-IV reactors. A detailed description of the reactor is presented Refs. [12].

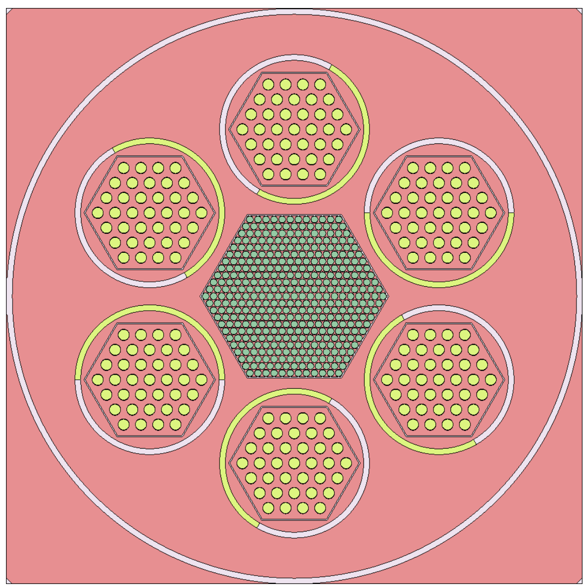

Figure 3: Radial view of the ELECTRA core showing the hexagonal fuel assembly made up of 397 fuel rods (center), the lead coolant (pink), the control assembly showing the six rotating control drums (the control rods are fully inserted inside the drums).

In Fig. 4, we present the neutron flux spectrum in the fuel as a function of neutron energy using the SERPENT code. The neutron flux in the fuel was estimated by defining a detector within the fuel material with user defined energy boundaries from 1e-5 to 20 MeV. SERPENT uses collision estimate of neutron flux for the calculation of reaction rates integrated over both space and energy [13]. As seen in the figure, the peak of the spectrum occurs at about 700 keV. The relatively hard spectrum allows for an efficient use of both the fissile and fertile isotopes within the ELECTRA core.

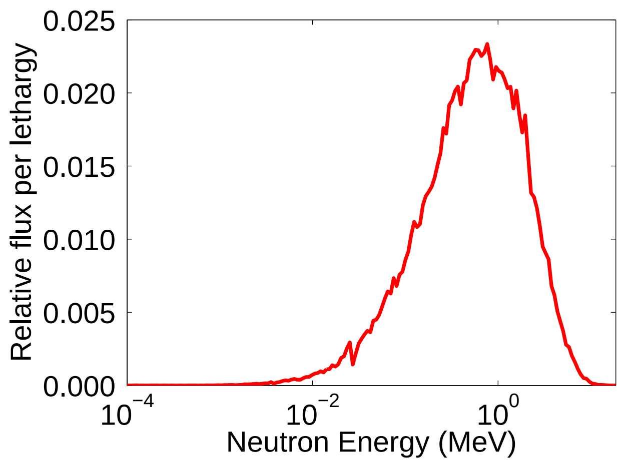

Figure 4: Neutron flux per lethargy in the fuel against neutron energy. The flux was normalized with the total flux. The peak of the spectrum occurs at about 700 keV.

2. Application

The TMC approach was utilized earlier in assessing the impact of ^{239}Pu cross section uncertainties on the full core 3-D SERPENT [22] model of the ELECTRA reactor at steady state [28] and in burnup calculations [29]. In this work however, we apply the TMC method for the propagation of nuclear uncertainties of the lead coolant (^{204,206,207,208}Pb) on the following four macroscopic parameters sensitive to nuclear data: the effective multiplication factor, the coolant temperature coefficient (CTC), the coolant void worth (CVW) and the effective delayed neutron fraction at zero burnup. For the computation of the CTC and the CVW, a perturbation in lead coolant density and a 100% void in the reactor were assumed respectively. The input files used in this study are the SERPENT geometry input file [12] and about 500 random ENDF files per isotope obtained from the TENDL project: ^{207,204}Pb from TENDL-2012 [18] and ^{208,206}Pb from

TENDL-2014 beta [17]. Each file consists of a unique set of nuclear data: resonance parameters, cross sections, angular distributions, double differential data and gamma production data.

All random files were converted into ACE format with the NJOY99.336 processing code [23]. Simulations were performed for the core at zero burnup with the absorber drums set at startup position and the control rods completely withdrawn. Criticality calculations were carried out for a total of 500 k_{eff} cycles with 50,000 neutrons per cycle corresponding to 25 million histories with an average statistical uncertainty of 22 pcm on the k_{eff}. This was done for a large set of ^{204,206,207,208}Pb random ENDF files to obtain distributions in k_{eff} values and other reactor parameters while maintaining all other isotopes as given in the JEFF-3.1 nuclear data library [14]. The standard deviation of each distribution in say the k_{eff} has two components: a) the statistical uncertainties in the Monte Carlo transport code used and b) the uncertainty due to nuclear data coming from the isotope varied. Consequently, the nuclear data uncertainty can be extracted for any parameter of interest as presented in Eq. (1).

3. Methodology

3.1. Convergence for k_{eff} distribution

To determine the convergence of the k_{eff} distribution, the first two moments of the distribution: the mean (right of Fig. 5) and the standard deviation $\sigma(k_{\mathrm{eff}}$ (left of Fig. 5) are presented as a function of random sampling of ^{208}Pb nuclear data. Even though a fluctuation in the probability distribution can be observed in both figures, its impact on the average k_{eff} and the standard deviation is small; a 1% variation on the standard deviation was observed.

3.2. Neutronic parameters

3.2.1. Effective multiplication factor (k_{eff})

The k_{eff} is an important parameter in criticality safety analysis. The impact of nuclear data uncertainty on reactor safety margins comes principally from uncertainty in criticality [30]. To quantify nuclear data uncertainties of the lead

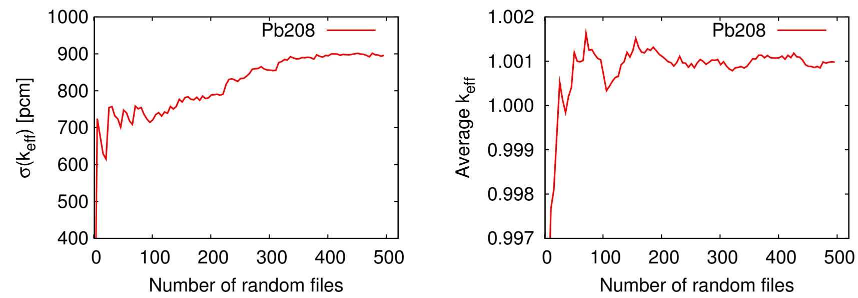

Figure 5: Example of convergence for the k_{eff} distribution in the case of varying ^{208}Pb nuclear. Two moments of the distribution are presented: the standard deviation, $\sigma(k_{eff})$ (left) and the mean (right).

coolant to the k_{eff},^{204,206,207,208}Pb nuclear data were varied while the k_{eff} was computed each time. In this way, distributions in the k_{eff} were obtained and the uncertainty due to nuclear data extracted using Eq.(1).

3.2.2. Coolant (Pb) temperature coefficient

The CTC is a balance between the positive contribution from hardening of the neutron spectrum and the reduction in neutron capture in the coolant, and the negative contributions from increase in leakage. The coolant temperature coefficient (CTC) was computed by assuming an increase in coolant temperature everywhere in the rector. The CTC was determined by performing criticality calculations with the SERPENT Monte Carlo code (version 1.1.17) [22] at two different coolant densities corresponding to the temperatures $T_1 = 600K$ and $T_2 = 1800K$ and then only varying the nuclear data of the following lead isotopes: ^{206}Pb, ^{207}Pb and ^{208}Pb. It must be noted here that, since the density effect is dominant in the CTC, all lead cross sections used in the calculation of the CTC were processed with the NJOY99.336 code at 600K. The temperature dependence of the coolant density (ρ^{Pb}) was calculated using Eq.(2) [11]:

$$\rho^{Pb}[kg/m^3] = 11367 - 1.1944 \times T \tag{2}$$

The temperature of the fuel was maintained at $1200K$ and the nuclear data library for all other isotopes except the isotope being varied was maintained as JEFF3.1. Coolant temperature coefficient which is the reactivity change per degree change in coolant temperature can be expressed as:

$$CTC = \frac{\Delta\rho}{\Delta T} \tag{3}$$

Where $\Delta\rho = \rho(T_1) - \rho(T_2)$ is the reactivity change and $\Delta T = T_1 - T_2$ is the the temperature change. Since the k_{eff} is close to 1.0 for both configurations, we can use $\Delta\rho = k_{eff}(T_1) - k_{eff}(T_2)$ for the reactivity change [31]. The CTC for a temperature change from T_1 to T_2 can therefore be expressed as:

$$CTC = \frac{k_{eff}(T_1) - k_{eff}(T_2)}{T_1 - T_2} \tag{4}$$

The nuclear data uncertainty in the CTC is propagated here similar to Eq.(1). If the statistical uncertainty on the k_{eff} at T_1 and T_2 are σ_{stat,T_1} and σ_{stat,T_2} respectively, then the combined statistical uncertainty ($\sigma_{stat,comb}$) for the computation of CTC can be expressed as:

$$\sigma^2_{stat,comb} = \sigma^2_{stat,T_1} + \sigma^2_{stat,T_2} \tag{5}$$

assuming that the statistical errors at T_1 and T_2 are uncorrelated. From the square of the total uncertainty (σ_{tot}) of the CTC distribution which is equal to quadratic sum of the nuclear data uncertainty (σ_{ND}) and the combined statistical uncertainty ($\sigma_{stat,comb}$), the uncertainty due to nuclear data can be extracted:

$$\sigma_{ND} = [\sigma^2_{tot} - \overline{\sigma^2_{stat,comb}}]^{1/2} \tag{6}$$

It should be noted that, since the difference between $k_{eff}(T_1)$ and $k_{eff}(T_2)$ is usually small, the CTC distribution can easily be dominated by statistics and hence longer computer hours are needed in the Monte Carlo simulations to obtain small statistical uncertainty; the usual rule of the thumb used for fast TMC is: $\sigma_{stat} \simeq 0.5 \times \sigma_{obs}$ [25].

3.2.3. Coolant Void worth

The Coolant void worth (CVW) which is the difference in reactivity between the flooded and voided primary vessel can be given by the expression:

$$CVW = \frac{k^{void}_{eff} - k^{flood}_{eff}}{k^{void}_{eff} . k^{flood}_{eff}} \tag{7}$$

Where, k_{eff}^{flood} and k_{eff}^{void} are the k_{eff} values for the flooded and voided cores, respectively. In order to investigate the impact of lead cross section uncertainties on the CVW, criticality calculations were performed for two different core configurations: 1) the voided vessel where all the lead was removed from the primary vessel and 2) for the core flooded with lead coolant. ^{204,206,207,208}Pb nuclear data were varied separately for the flooded vessel while maintaining the nuclear data for all other isotopes as JEFF-3.1. Applying Eq.(7) for each isotope, distributions of CVW were obtain.

The voided vessel involves only one SERPENT code calculation, consequently, only the statistical uncertainty of the flooded vessel (σ_{stat}^{flood}), is used in Eq.(1), when σ_{ND} is calculated. However, the σ_{stat}^{void} will introduce a bias in the mean value of the CVW and therefore the 100 % voided vessel is calculated with high statistical precision. Since the spread is only dependent on data from the flooded reactor, we can approximate the nuclear data uncertainty of the CVW ($\sigma_{CVW,ND}$) as:

$$\sigma_{CVW,ND} \approx \frac{\sigma_{k_{\text{eff}},ND}^{flood}}{k_{\text{eff}}^{flood}.k_{eff}^{void}} \tag{8}$$

However, Eq. 8 was not used for the calculation of $\sigma_{CVW,ND}$ in this work. The actual spread of the CVW was used.

3.2.4. Effective delayed neutron fraction

The effective delayed neutron fraction (β_{eff}) is important for reactor transient analysis. To investigate the impact of nuclear data uncertainties of lead on the β_{eff}, the Serpent Monte Carlo code was simulated with each random ACE file after setting the fuel temperature to $1200K$ and the coolant temperature to $600K$ in the ELECTRA input file. The values of the effective delayed neutron fraction together with the relative uncertainties were obtained directly from the main SERPENT output file. The total effective delayed neutron fraction can be expressed as [32]

$$\beta_{eff} = \frac{k_{eff} - k_p}{k_{eff}} \tag{9}$$

Where k_{eff} is the eigenvalue for all neutrons produced and k_p is the eigenvalue for prompt neutrons only. Distributions in β_{eff} were obtained by varying $^{204,206,207,208}Pb$ nuclear data only. Using Eq.(1), nuclear data uncertainties were extracted from the various distributions.

3.3. Uncertainty of the Uncertainty

For more accurate integral results for the improvement of current design and for GEN-IV reactor development, it is important to study the accuracy of the calculated uncertainty. This can be achieved by quantifying the uncertainty on the estimated nuclear data uncertainty. The uncertainty of the uncertainty due to nuclear data ($\triangle\sigma_{ND}$) can be given by the expression:

$$\triangle\sigma_{ND} = \frac{\triangle V_{ND}}{2\sigma_{ND}} \tag{10}$$

Where V_{ND} is the variance due to nuclear data and Δ is the associated uncertainty. $\triangle V_{ND}$, the uncertainty of the variance of nuclear data is given by:

$$\triangle V_{ND} = [(\triangle V_{obs})^2 + (\triangle V_{stat})^2]^{1//2} \tag{11}$$

Where V_{obs} is the variance in the observed parameter, V_{stat} is the variance due to statistics. The uncertainty of the uncertainty calculation for nuclear data uncertainty analysis has been presented in more detail in Ref. [26]. In this paper, the method assuming a normal distribution was used.

3.4. Partial variations

In the previous section, methods for computing the global uncertainties due to nuclear data for some reactor parameters were presented. However, to quantify the contributions of different reaction channels or parts of the ENDF file to the global uncertainties obtained, we introduced the concept of partial variation. This involves, evaluating the relationship between specific cross sections and a particular response parameter of interest after controlling for some partial cross sections or other variables within the ENDF file. This was achieved by perturbing parts of the ENDF files while keeping other parts constant to generate a new set of random files. The parts of the ENDF file perturbed include: the elastic scattering (n, el), inelastic scattering (n, inl) neutron capture (n, γ), $(n, 2n)$, resonance parameters and angular distributions. To investigate the impact of only resonance parameters on reactor parameters for instance, only MF2 (in ENDF nomenclature) was perturbed. This means that, each complete ENDF file then contain a unique set of resonance parameters such as the scattering radius, the average level spacing and the average reduced neutron width. Similar for the (n,el) cross section, MF3, MT2 was kept constant and different parts of the ENDF file were varied. To accomplish this, the first file (i.e run zero of the random files obtained from the TENDL-2012 [18]) was kept as the unperturbed file while different sections of the random ENDF files were perturbed and a unique set of random files produced. All the perturbed random files were then processed into ACE files with the NJOY processing code at 600K and used in the SERPENT code for reactor core calculations. Thus, the variance of the observable (reactor quantity of interest) due to the partial variation ($\sigma^2_{(n,x_n),obs}$) can be expressed as:

$$\sigma^2_{(n,x_n),obs} = \sigma^2_{(n,x_n),ND} + \overline{\sigma^2_{stat}} \tag{12}$$

Where $\overline{\sigma^2_{stat}}$ is the mean value of the variance due to statistics and $\sigma^2_{(n,x_n),ND}$ is the variance due to nuclear data as a result of partial variation and $(n, x_n) =$ (n, γ), (n, el), (n, inl), $(n, 2n)$, resonance parameters or angular distributions. In this way, the nuclear data uncertainties due to a specific reaction channel or a specific part of the ENDF file were studied and quantified.

In Fig. 6, the perturbed random ACE ^{208}Pb cross sections are plotted as a function of incident neutron energy. In the top left and top right, the (n,el) and (n,γ) cross sections are presented respectively, after perturbing only resonance parameter data. As can be observed, the partial variation of only resonance parameters, affect both ^{208}Pb(n,el)(top left) and ^{208}Pb(n,γ) (top right)cross sections from thermal up to about 1 MeV. The boundary between the resolved resonance region and the high energy region for ^{208}Pb random files is at about 1 MeV. In the TENDL library, the unresolved resonance region parameters and the cross sections in the high energy region are generally calculated using the optical model implemented within the TALYS code [19]. Since ^{208}Pb has no resonances in the low energy region, the observed spread in the (n,el) and (n,γ) cross sections can be attributed to the variation of the scattering radius. The scattering radius is an important parameter required for the computation of the scattering and total cross sections [15]. In the bottom left and bottom right of Fig. 6, the ^{208}Pb(n,el) and ^{208}Pb(n,γ) are presented for the partial variation of the (n,el) cross section in the fast energy range (above 1 MeV) respectively. A spread is observed above 1 MeV for the partial variation of ^{208}Pb(n,el) cross section (bottom left) as can be observed from the figure. Since results in the fast energy region is obtained from TALYS, the spread can be attributed to the variation of model parameters within the TALYS code. The lack of spread observed for the (n,γ) is not surprising as the variation of the (n,el) cross section has no significant impact on the (n,γ) cross section.

3.5. Correlations

3.5.1. Cross sections and parameter correlations

It is of interest in nuclear reactor physics and criticality analyses to study the correlations and sensitivities between various cross sections and a particular response parameter. In this study, we used a sensitivity method based on the Monte Carlo evaluation developed at Nuclear Research and Consultancy Group (NRG) [24] to study the correlations between different cross sections and the k_{eff} for the ELECTRA reactor. Using a set of random files for a specific isotope, correlation factors are computed between a parameter of interest and a partial cross section averaged over a specific energy group:

$$\rho_{xy} = \frac{\sum_{i=1}^{n}(x_i - \overline{x})(y_i - \overline{y})}{(n-1)s_x s_y} \tag{13}$$

Where x_i is the random cross section, $\overline{x}$ is the cross section mean value for the energy group, y_i is the parameter value for the i^{th} random file, $\overline{y}$ is the mean parameter value, s_x and s_y are their sample standard deviations. The correlation coefficient (ρ_{xy}) which is a measure of the strength of the linear dependence

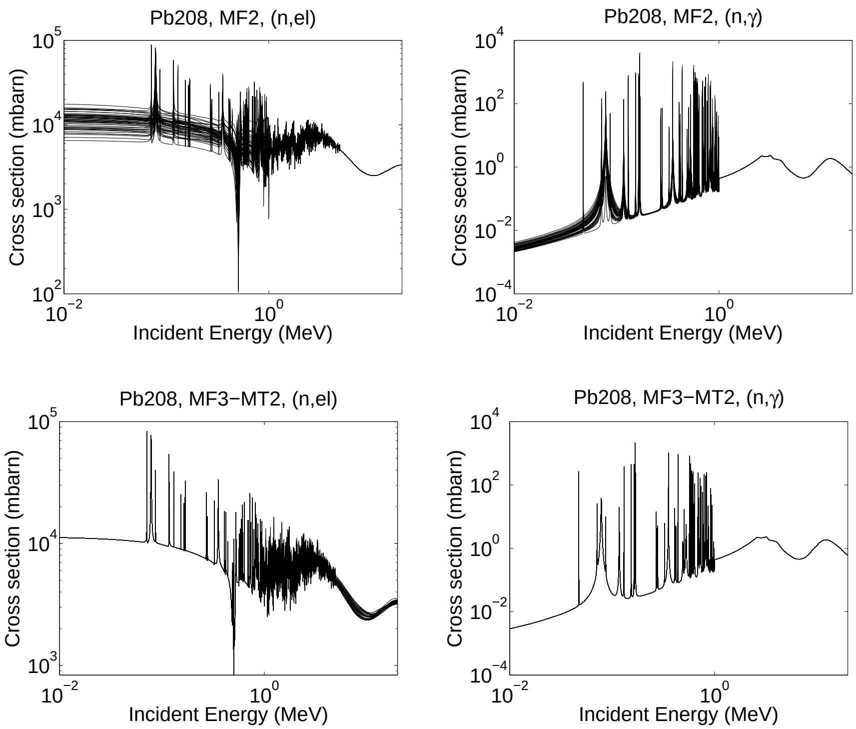

Figure 6: Random ACE ^{208}Pb cross sections plotted as a function of incident neutron energy. For Top left: ^{208}Pb(n,el) and top right: ^{208}Pb(n,γ), only MF2 (resonance parameters) were varied while for bottom left: ^{208}Pb(n,el) and bottom right: ^{208}Pb(n,γ), only the elastic scattering cross sections in the fast energy range were varied.

between two variables, varies between +1 and -1. Using Eq.(13), correlation factors were calculated between k_{eff} and four partial cross sections: elastic scattering (n, el), inelastic scattering (n, inl), neutron capture (n, γ), $(n, 2n)$ averaged over 44 energy groups. In Fig. 7, we present a flow chart diagram which represents how the cross section-parameter correlations computation was carried out. Random files obtained from the TENDL project were first linearized using the LINEAR module, reconstructed from resonance parameters using the RECENT module and then Doppler broadened using the SIGMA1 module of the PREPRO processing code [33]. The cross sections were finally collapsed into 44 energy groups using the GROUPIE module. The correlation factors obtained between the k_{eff} and different energy groups were plotted against incident neutron energy and observations made. A more detailed presentation of this methodology can be found in Refs. [19, 24]. In Fig. 8, we present correlation plots between ran-

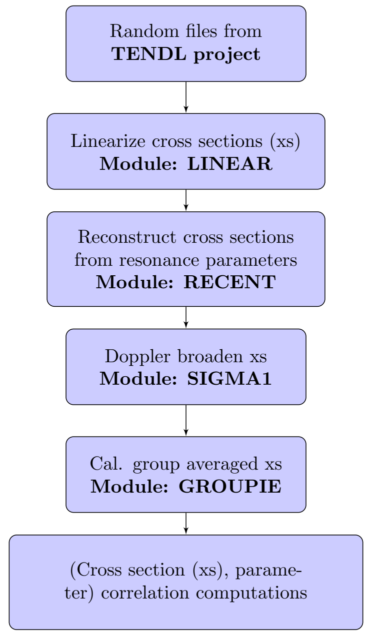

Figure 7: Cross section-parameter correlation flow chart diagram. Correlation factors are computed by randomly changing cross sections for given incident neutron energies.

dom elastic scattering cross sections and incident neutron energy for two energy groups (25-100keV and 2.48-3MeV), against the k_{eff} after varying only ^{208}Pb nuclear data. The correlation factors computed here are inserted in Fig. 13, where correlations for all 44 energy groups are presented. A high correlation coefficient ($\rho_{xy} = 0.67$) is recorded for the k_{eff} against ^{208}Pb(n,el) at 25-100 keV energy group, signifying a strong relationship between the elastic scattering cross section between the 25-100keV energy group and the k_{eff} while the weak correlation coefficient observed for the ^{208}Pb(n,el) cross section at 2.48-3MeV energy group implies a weak relationship between ELECTRA and the ^{208}Pb(n,el) cross section for that energy range.

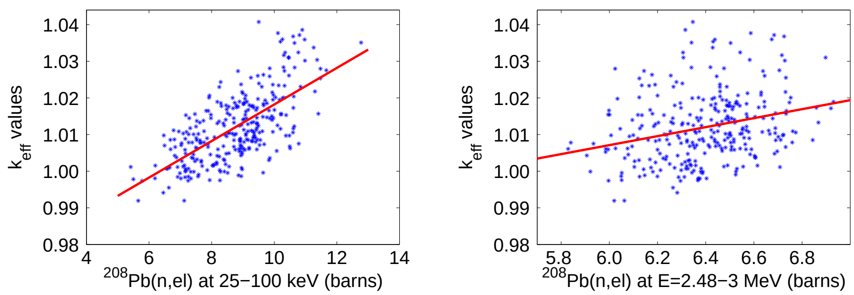

Figure 8: Correlation between k_{eff} and the elastic scattering cross section averaged over 25-100 keV energy range (correlation coefficient $(\rho_{xy}) = 0.67$) (left) and, k_{eff} against the elastic scattering cross section averaged over the 2.48-3 MeV energy range with a correlation coefficient $(\rho_{xy}) = 0.27$ (right) obtained by varying ^{208}Pb nuclear data.

3.5.2. Energy - energy correlations

As a result of using theoretical models in TALYS, the impact of energy-energy correlations for a given cross section could be quite strong [19] and could therefore have strong influences on the (parameter, cross section) correlations computed. Hence, the influence of energy-energy correlations on the correlations computed from the previous section was also investigated. Correlation factors between random cross sections for a particular reaction channel are computed at two specific incident neutron energy groups. This was done for different energy groups between 0.01 to about 8 MeV for the elastic scattering (n, el) cross sections of ^{204,206,207,208}Pb. In Fig. 9, the energy-energy correlation examples are presented for ^{208}Pb random elastic cross sections for the 25-100 keV against 2.48-3 MeV (left) and for the 1.85-2.35 MeV against 2.48-3 MeV (right) energy groups respectively. Each correlation factor calculated represents an energy bin as presented in the energy - energy correlation matrix in Fig. 14. As it can be seen from the Fig. 9, a weak correlation $(\rho_{xy}) = 0.0026$) is observed for the 2.48-3 MeV against 25-100 keV (left). A relatively strong correlation coefficient (ρ_{xy} = 0.76) is however observed for the 1.85-2.35 MeV against 2.48-3 MeV (right) energy group. These energy-energy correlations influence the cross section - parameter correlations discussed in section 3.5.1.

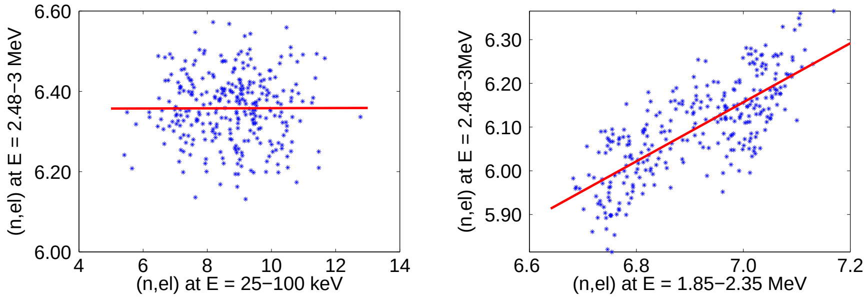

Figure 9: Examples of energy-energy correlations for random ^{208}Pb elastic between 25-100 keV and 2.48-3 MeV (correlation coefficient $(\rho_{xy}) = 0.0026$) (left) and, between 1.85-2.35 MeV and 2.48-3 MeV energy groups (correlation coefficient $(\rho_{xy}) = 0.76$) (right).

4. Results and Discussion

4.1. Global uncertainties

In Fig. 10, probability distributions for the k_{eff} are presented for varying ^{208,207,206,204}Pb nuclear data. It can be observed that, the k_{eff} distribution for ^{208}Pb, ^{207}Pb and ^{206}Pb slightly deviate from Gaussian distribution with tails in the high k_{eff} region. Skewness values of 0.58, 0.37 and 0.33 were observed for the ^{208}Pb, ^{207}Pb and ^{206}Pb distributions (see Table 5). The non-Gaussian distribution observe for ^{208}Pb and ^{207}Pb distributions is not surprising as asymmetric k_{eff} distribution due to some lead isotopes has been reported earlier [9, 10]. In the studies([9, 10]), k_{eff} distributions for 14 fast benchmarks deviated from Gaussian distribution to the extent that a better fit was obtained with the Extreme Value Theory(EVT) curve. The asymmetric behavior was attributed to the shape of the inelastic and capture cross section distributions [9]. But in our case, the deviation is related to the shape of the elastic scattering cross sections, the resonance parameter variation and the angular distributions as can be observed in Fig. 12. Our best estimate (mean value) of the k_{eff} for varying ^{208}Pb nuclear data was 1.00098±0.0002 (statistical uncertainty), for ^{207}Pb was 1.00367±0.0002, for ^{206}Pb was 1.00164±0.00021 and 1.00015±0.0002 for ^{204}Pb nuclear data variation were compared to 1.00307±0.0003 obtained with JEFF3.1 [14] nuclear data library. The differences observed can be attributed to the uncertainty in nuclear data. Since the large uncertainties observed are related to the central values used for randomizing the nuclear data used, further work is recommended as feedback to model calculations for these isotopes.

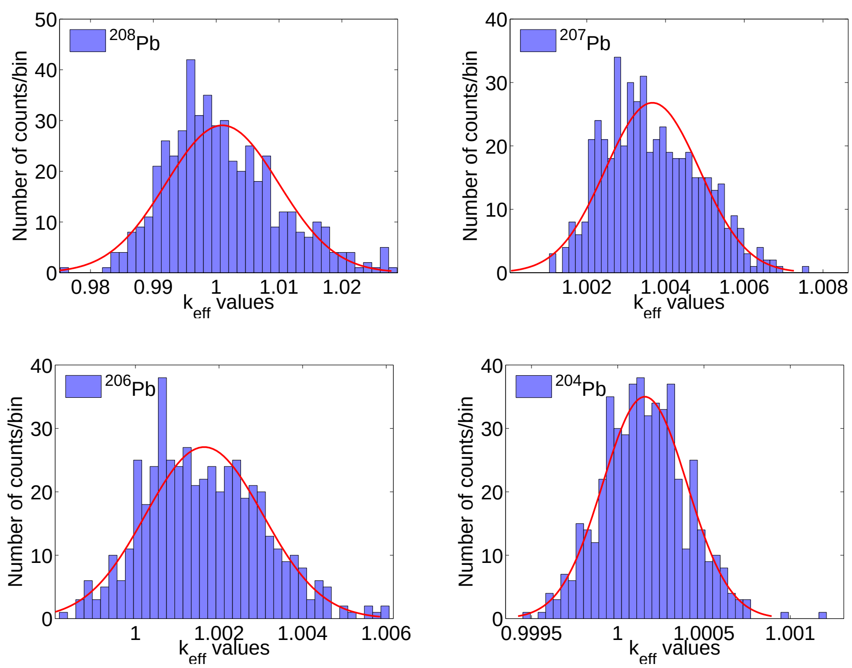

Figure 10: k_{eff} distribution for ELECTRA for varying lead nuclear data at 600 K coolant temperature. Top left: ^{208}Pb, top right: ^{207}Pb, bottom left: ^{206}Pb and bottom right: ^{204}Pb. The k_{eff} distribution for ^{208}Pb and ^{207}Pb slightly deviate from Gaussian distribution with tails in the high k_{eff} region. Random ENDF files for ^{207}Pb and ^{204}Pb were obtained from TENDL-2012 [18] whiles ^{208}Pb and ^{206}Pb were produced in this work and can be obtained from TENDL-2014 beta [17].

The global CVW distribution for varying ^{208,207,206,204}Pb nuclear data are presented in Fig. 11. A deviation from the Gaussian distribution was observed with a tail in the low CVW region for all the isotopes with negative skewness values. A negative skewness value which implies a tail of CVW towards negative values is good for reactor safety. A positive skewness value would have had safety implications. A high uncertainty value of 896 pcm due to ^{208}Pb nuclear data is observed. This can be attributed to the relatively high uncertainties of the $^{208}\mathrm{Pb}(n, el)$ cross section, resonance parameters and the angular distributions (see next section). Since the CVW is a difference in the eigenvalues between two reactor states, the large uncertainty in the k_{eff} observed due to ^{208}Pb was propagated all the way through. Even though the lead boiling scenario mostly

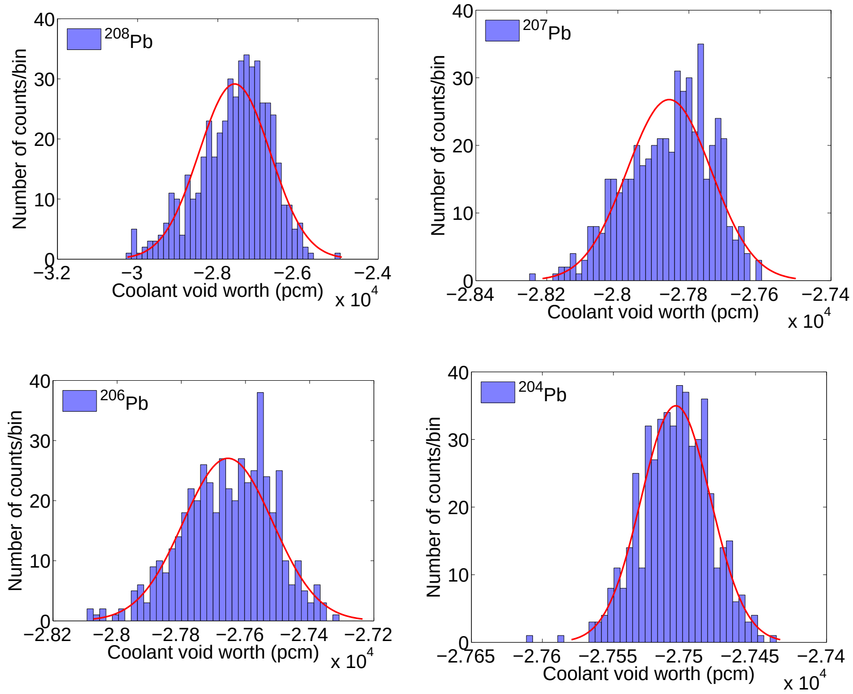

Figure 11: Coolant void worth (CVW) distribution for ELECTRA for varying lead nuclear data. Top left: ^{208}Pb, top right: ^{207}Pb, bottom left: ^{206}Pb and bottom right: ^{204}Pb. The CVW distribution for all the lead isotopes deviate slightly from the Gaussian distribution with tails in the low CVW region. Random ENDF files for ^{207}Pb and ^{204}Pb were obtained from TENDL-2012 [18] whiles ^{208}Pb and ^{206}Pb were obtained from TENDL-2014 beta [17].

assumed in coolant void worth computations can be considered as unreal in lead Fast Reactors (LFRs) because of the high boiling point of the lead coolant (1749 ^oC) which is far from the common reactor coolant operating temperatures [11], potential mechanism such as a rupture in the heat exchange system may cause an even distribution of small bubbles within the coolant which could trigger power oscillations. A detailed study on causes of density changes on ELECTRA has been presented in Ref. [34]. In Table 2, the global nuclear data uncertainties together with their uncertainties for ^{204,206,207,208}Pb are presented for the k_{eff}, the effective delayed neutron fraction, the coolant temperature coefficient, and the coolant void worth. Large uncertainties in the k_{eff} were observed for ^{208}Pb

Table 2: Nuclear data uncertainty (global) in reactor parameters for ELECTRA, varying only ^{204,206,207,208}Pb nuclear data. The results are all given in pcm. The values quoted in the sixth row are values obtained from the quadratic sum of the ND uncertainties coming from ^{204,206,207,208}Pb ($\sigma_{ND,Pb,tot}$). It was assumed that the uncertainties were uncorrelated. it should be noted that, to obtain the ND uncertainty for the CTC in pcm/K, the value must be divided by the difference in temperature (1200K). Random ENDF files for ^{207}Pb and ^{204}Pb were obtained from TENDL-2012 [18] whiles ^{208}Pb and ^{206}Pb were obtained from TENDL-2014 beta [17].

Isotopes	$\sigma_{ND}(k_{eff})$	$\sigma_{ND}(CTC)$	$\sigma_{ND}(CVW)$
^{208}Pb	896±28	61±2	890±28
^{207}Pb	118±4	-	117±4
^{206}Pb	136±5	-	136±5
^{204}Pb	12±2	-	12±2
Total($\sigma_{ND,Pb,tot}$)[pcm]	914	61	907
Relative uncertainties (%)	0.9	2.6	3.3

indicating that, the ELECTRA core is highly sensitive to ^{208}Pb nuclear data variation and hence its uncertainties. Relatively large uncertainties in the k_{eff} were recorded for ^{206}Pb and ^{207}Pb. The uncertainty from the ^{204}Pb was however, small. Since the β_{eff} is not very sensitive to lead nuclear data variation, a bulk of the spread in the distribution came from statistics and consequently, the uncertainty of uncertainty of nuclear nuclear data obtained was found to be quite large, therefore no proper estimate of the nuclear data uncertainty could be obtained. The observed spread in the CTC for ^{204,206,207}Pb was dominated by statistics. Except for ^{204}Pb, the impact of nuclear data uncertainty for all lead isotopes on the CVW were relatively high.

4.2. Partial variation of nuclear data

The impact and contribution of partial channels on the nuclear data uncertainty observed on the k_{eff} and the CVW were further studied and quantified for some partial cross sections and are presented in Tables 3 and 4 together with their uncertainties. Since the global impact of ^{204}Pb was relatively small, partial variations were carried out only for ^{206,207,208}Pb. In Figs. 12, we present the distribution in k_{eff} for varying elastic scattering, resonance parameters, angular distributions and neutron capture cross sections of ^{208}Pb. Non Gaussian shapes

Table 3: Nuclear data uncertainty in k_{eff} due to partial variations of ^{206,207,208}Pb nuclear data. Since the global impact of the ^{204}Pb nuclear data uncertainty was relatively small as can be observed from Table 2 therefore, no partial variation was performed for ^{204}Pb. All lead files used here were obtained from TENDL-2012 [18].

	^{208}Pb	^{207}Pb	^{206}Pb
Nuclear data varied	$\sigma_{ND}(k_{eff})$[pcm]	$\sigma_{ND}(k_{eff})$[pcm]	$\sigma_{ND}(k_{eff})$[pcm]
n, el	289±12	58±3	50±2
$n, 2n$	7±3	4±6	5±4
n, γ	83±4	10±2	10±2
n, inl	8±3	30±2	23±2
Resonance parameters	862±35	55±3	145±6
Angular distributions	226±9	101±4	107±5

Table 4: Nuclear data uncertainty in CVW due to partial variations of ^{206,207,208}Pb nuclear data. Since the global impact of the ^{204}Pb nuclear data uncertainty was relatively small as can be observed from Table 2 therefore, no partial variation was carried out for ^{204}Pb. All lead files used here were obtained from TENDL-2012 [18]. The similarity in results observed between the CVW and the k_{eff} results in Fig. 3 is expected since the CVW is the difference in the eigenvalues between two reactor states.

	^{208}Pb	^{207}Pb	^{206}Pb
Nuclear data varied	$\sigma_{ND}(CVW)$[pcm]	$\sigma_{ND}(CVW)$[pcm]	$\sigma_{ND}(CVW)$[pcm]
n, el	283±12	58±3	48±2
$n, 2n$	6±3	3±7	3±7
n, γ	82±4	10±2	9±2
n, inl	7±3	30±2	22±2
Resonance parameters	837±34	55±3	142±6
Angular distributions	224±9	101±4	104±4

are observed for the variation in the elastic scattering, resonance parameters and the angular distributions with skewness values are presented in Table 5. High tails were observed in the high k_{eff} regions for the elastic scattering cross section and the resonance parameter variations. A tail in the low k_{eff} region was however observed for the angular distributions. In Table 5, the skewness values of k_{eff} distributions for the partial variation of ^{208,207,206}Pb are presented. High skewness values are recorded for ^{207}Pb and ^{206}Pb (n,el) cross sections as can be observed from the table. The bulk contribution to the nuclear data uncertainty

Table 5: Table showing the skewness values for the k_{eff} distribution due to partial variation of ^{208,207,206}Pb nuclear data.

	Skewness values		
k_{eff}	^{208}Pb	^{207}Pb	^{206}Pb
Resonance parameters	0.75	0.12	-0.31
(n,el) cross section	0.98	0.86	0.73
Angular distributions	-0.48	-0.18	-0.16
(n.γ) cross section	0.08	-0.12	0.04
Global k_{eff}	0.58	0.37	0.33

on the k_{eff} and the CVW come from uncertainties in the resonance parameters, the elastic scattering cross section (since the correlation between this cross section and ELECTRA is relatively high for ^{206,207,208}Pb) and from the angular distributions. Uncertainties due to $(n, 2n)$ and (n, inl) were found to be small for all isotopes. The impact from the (n, γ) on the k_{eff} was also observed to be small as expected since fast reactors like ELECTRA, generally have small fraction of capture reactions in the core.

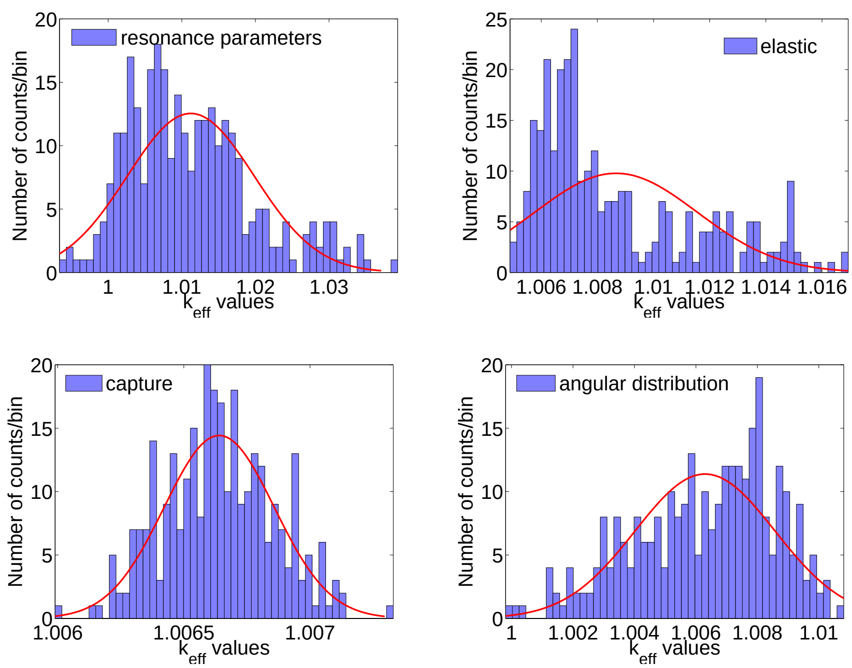

Figure 12: k_{eff} distribution for ELECTRA for varying resonance parameters only (top left), elastic scattering only (top right), neutron capture only (bottom left) and angular distributions only (bottom right) of ^{208}Pb.

4.3. Cross sections and parameter correlations

In Figs. 13, we present (cross section - k_{eff}) correlations for four partial channels as a function of incident neutron energy for all the lead isotopes under studied. The partial channels presented are the (n,γ), (n, el), (n, inl) and $(n, 2n)$ cross sections. Each bin in Fig. 13, represents correlation factors plotted between the k_{eff} and a particular cross section for a particular energy group as presented earlier in Fig. 8. It should be noted here that, since the cross section of the random ENDF files used here were reconstructed with the RECENT module and Doppler broadened using the SIGMA1 modules of the PREPRO code as presented earlier in section 3.5, the resonance contributions were included in the cross sections and hence in the correlations computed.

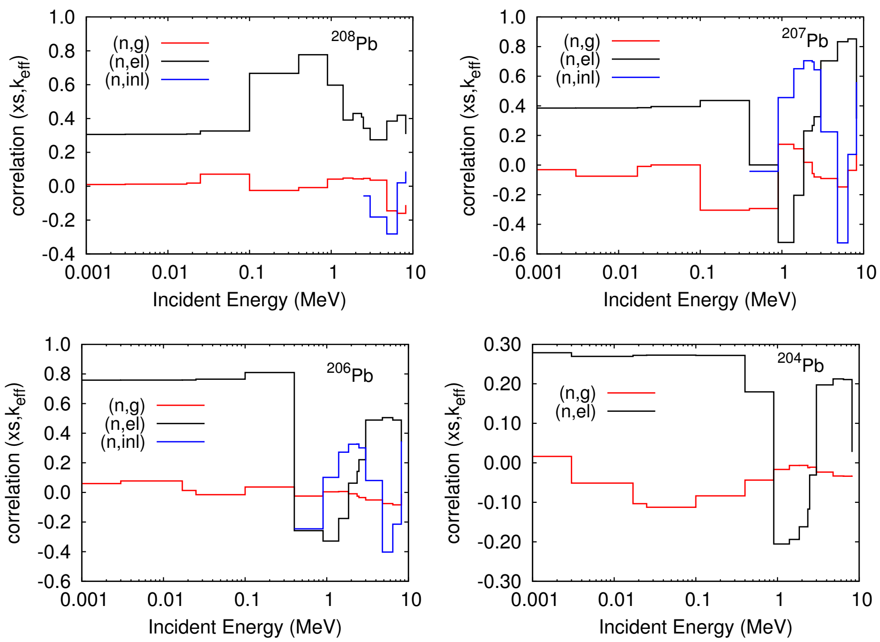

Figure 13: k_{eff} sensitivity to lead cross sections for ELECTRA reactor. Correlation factors obtained between four particular cross section and the k_{eff} are plotted against incident energies. Top left: ^{208}Pb, top right: ^{207}Pb, bottom left: ^{206}Pb and bottom right: ^{204}Pb. Each bin represents correlation factors computed between the k_{eff} and a particular reaction channel for a particular energy group as presented in earlier in Fig. 8.

From Fig. 13, a strong correlation is observed for the $^{208}\mathrm{Pb}(n, el)$ cross section between 0.5 and about 1.0 MeV. This is expected as ^{208}Pb contains high peak elastic scattering resonances between the 10^{-2} and 5 MeV energy range. Since ELECTRA is a fast reactor, the $^{208}\mathrm{Pb}(n, \gamma)$ cross section was found to be weakly correlated as expected. This was also observed for the (n,2n) channel (not shown in the figure). This was expected, since the $^{208}\mathrm{Pb}(n, 2n)$ channel opens at about 7.5 MeV which is well above the peak of the neutron spectrum of ELECTRA (700 keV). The ^{208}Pb(n, inl) cross section was also observed to be weakly correlated. For ^{207}Pb, as can be observed from Fig. 13, strong correlations can be observed for the ^{207}Pb(n, el) cross sections from about 1.0 to 10 MeV. This could be attributed to the ^{207}Pb elastic scattering resonance peaks which occur between the energy range: 10^{-2} and 5 MeV. Also, high correlations are observed for ^{207}Pb(n, inl) cross section between about 1 to 5 MeV. However, the ^{207}Pb$(n, 2n)$ and the ^{207}Pb(n, γ) cross sections had weak correlations. From the same diagram, relatively high correlations were observed for the ^{206}Pb(n, el) and the ^{206}Pb(n, inl) cross sections. The ^{206}Pb(n, γ) and the ^{206}Pb$(n, 2n)$ cross sections were however observed to have weak correlations with ELECTRA. For ^{204}Pb, weak correlations are observed for ^{204}Pb(n, el) and ^{204}Pb(n, γ) cross sections but no correlations were however observed for the ^{204}Pb(n, inl) and ^{204}Pb$(n, 2n)$ cross sections. As can be seen in Fig. 13, relatively strong correlations can be observed for the (n,el) cross section at low incident energies for all the lead isotopes. This can be attributed to the energy-energy correlations discussed earlier in section 3.5.2 and presented in Fig. 14. Energy-energy correlations can come from using the same theoretical models and the same computer codes in the calculations of random cross sections. In Fig. 14, we present the

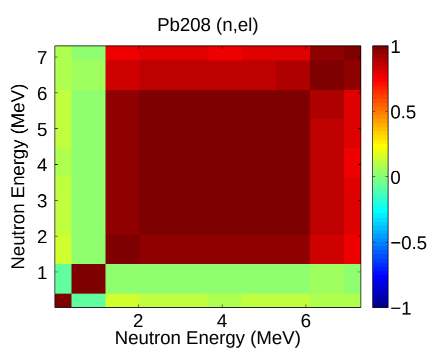

Figure 14: Energy - energy cross section correlation example for ^{208}Pb(n,el)

energy - energy correlation matrix for ^{208}Pb (n, el) cross sections for averaged group cross sections between the 0.1 to 8 MeV energy range showing the diagonal and off diagonal elements. Strong energy correlations can be observed at high energies. As an improvement, we plan to investigate in more detail, the impact of these energy-energy correlations on the cross section-parameter correlations observed, in a separate paper.

5. Conclusions

Uncertainty propagation was carried out to study the impact of nuclear data uncertainties of lead isotopes ^{204}Pb, ^{206}Pb, ^{207}Pb and ^{208}Pb on the European Lead Training Reactor (ELECTRA) using the Total Monte Carlo approach. A 0.9% and 3.3% uncertainty due to lead nuclear data were obtained on the k_{eff} and CVW respectively. It was observed that the uncertainty in the k_{eff} for all the isotopes except for ^{204}Pb were large with significant contribution coming from ^{208}Pb. The dominant contributions to the uncertainty in the k_{eff} came from uncertainties in the resonance parameters for ^{208}Pb; however, elastic scattering cross section and the angular distributions also had significant impacts. The nuclear data uncertainty on the β_{eff} for all the isotopes was found to be small. Nuclear data uncertainty due to ^{208}Pb on the coolant void worth and for the coolant temperature coefficient was found to be significantly large and dominated by the uncertainty in the resonance parameters. A Monte Carlo sensitivity based method was used to study the cross section-parameter correlations between some reactor parameters and partial cross sections. Strong correlations were observed between the k_{eff} and (n, el) cross section for all the isotopes studied over the entire energy spectra. It was also observed that energy-energy correlations could be such strong that, they could influence the cross section-parameter correlations and should therefore be investigated further.

6. Acknowledgment

This work was done with financial support from the Swedish Research Council through the GENIUS project.

References

[1] H. Sjöstrand, E. Alhassan, S. Conroy, J. Duan, C. Hellesen, S. Pomp, M. Österlund, A. Koning, D. Rochman, Total Monte Carlo evaluation for dose calculations, Radiation protection dosimetry (2013).

[2] R. A. Forrest, The role of nuclear data for fusion technology studies, Nuclear Engineering and Design 241 (10) (2011) 4326–4330.

[3] D. Rochman, A. Koning, S. C. V. D. Marck, A. Hogenbirk, C. Sciolla, Nuclear data uncertainty propagation: Perturbation vs. monte carlo, Annals of Nuclear Energy 38 (5) (2011) 942–952.

[4] W. Zwermann, B. Krzykacz-Hausmann, L. Gallner, A. Pautz, M. Mattes, Uncertainty analyses with nuclear covariance data in reactor core calculations, Journal of the Korean Physical Society 59 (2) (2011) 1256–1259.

[5] C. Gustavsson, S. Pomp, H. Sjöstrand, G. Wallin, M. Österlund, Massive computation methodology for reactor operation (macro), in: Proceedings of the European Nuclear Conference (ENC 2010), Barcelonna, Spain, May 2 - June 2, 2010.

[6] G. Aliberti, G. Palmiotti, M. Salvatores, T. Kim, T. Taiwo, M. Anitescu, I. Kodeli, E. Sartori, J. Bosq, J. Tommasi, Nuclear data sensitivity, uncertainty and target accuracy assessment for future nuclear systems, Annals of Nuclear Energy 33 (8) (2006) 700–733.

[7] J. Briesmeister, MCNP - a general Monte Carlo n-particle transport code, version 4c, Tech. rep. LA-13709-M, Los Alamos National Laboratory, Los Alamos New Mexico, USA, 2000.

[8] A. J. Koning, S. Hilaire, M. Duijvestijn, TALYS-1.0:Making nuclear data libraries using TALYS, in: Proceedings of the International Conference on nuclear data for science and technology, 2007, pp. 211–214.

[9] A. J. Koning, D. Rochman, Towards sustainable nuclear energy: Putting nuclear physics to work, Annals of Nuclear Energy 35 (2008) 2024–2030.

[10] D. Rochman, A. J. Koning, S. van der Marck, Uncertainties for criticality-safety benchmarks and k_{eff} distributions, Annals of Nuclear Energy 38 (2009) 942–952.

[11] L. Cinotti, C. F. Smith, C. Artioli, G. Grasso, G. Corsini, Lead-Cooled Fast Reactor (LFR) Design: Safety, Neutronics, Thermal Hydraulics, Structural Mechanics, Fuel, Core, and Plant Design, Springer Science+BusinessMedia, 2010.

[12] J. Wallenius, E. Suvdantsetseg, A. Fokau, ELECTRA: European Lead-Cooled Training Reactor, Nuclear Technology 177 (12) (2012) 303–313.

[13] J. Leppänen, Psg2/serpent - a continuous-energy monte carlo reactor physics burnup calculation code. vtt technical research centre of finland, User manual.

[14] A. Koning, R. Forrest, M. Kellett, R. Mills, H. Henriksson, Y. Rugama, The JEFF-3.1 nuclear data library, JEFF report 21.

[15] M. Chadwick, M. Herman, P. Obložinskỳ, M. E. Dunn, Y. Danon, A. Kahler, D. L. Smith, B. Pritychenko, G. Arbanas, R. Arcilla, et al., ENDF/B-VII. 1 nuclear data for science and technology: cross sections, covariances, fission product yields and decay data, Nuclear Data Sheets 112 (12) (2011) 2887–2996.

[16] K. Shibata, O. Iwamoto, T. Nakagawa, N. Iwamoto, A. Ichihara, S. Kunieda, S. Chiba, K. Furutaka, N. Otuka, T. Ohasawa, et al., JENDL-4.0: a new library for nuclear science and engineering, Journal of Nuclear Science and Technology 48 (1) (2011) 1–30.

[17] A. Koning, D. Rochman, S. van der Marck, J. Kopecky, J. C. Sublet, S. Pomp, H. Sjöstrand, R. Forrest, E. Bauge, H. Henriksson, O. Cabellos,

S. Goriely, J. Leppanen, H. Leeb, A. Plompen, R. Mills, Tendl-2014: Talys-based evaluated nuclear data library, www.talys.eu/tendl-2014.html (2014).

[18] A. Koning, D. Rochman, S. van der Marck, J. Kopecky, J. C. Sublet, S. Pomp, H. Sjöstrand, R. Forrest, E. Bauge, H. Henriksson, Tendl-2012: Talys-based evaluated nuclear data library, www.talys.eu/tendl-2012.html (2012).

[19] A. J. Koning, D. Rochman, Modern nuclear data evaluation with TALYS code system, Nuclear Data Sheets 113 (2012) 2841–2934.

[20] D. Rochman, TARES-1.1: Generation of resonance data and uncertainties, User manual, Nuclear Research and Consultancy Group (NRG), unpublished, 2011.

[21] A. J. Koning, TEFAL-1.26: Making nuclear data libraries using TALYS, User manual, Nuclear Research and Consultancy Group (NRG), unpublished, 2010.

[22] J. Leppänen, Development of a New Monte Carlo Reactor Physics Code, D.Sc. Thesis, Helsinki University of Technology, 2007.

[23] R. MacFarlane, A. Kahler, Methods for processing ENDF/B-VII with NJOY, Nuclear Data Sheets 111 (12) (2010) 2739–2890.

[24] D. Rochman, A. J. Koning, D. F. D. Cruz, Uncertainties for the Kalimer Sodium Fast Reactor: Void reactivity coefficient, k_{eff}, β_{eff}, depletion and radiotoxity, Nuclear Science and Technology 48 (8) (2011) 1193–1205.

[25] D. Rochman, W. Zwermann, S. van der Marck, A. J. Koning, H. Sjöstrand, P. Helgesson, B. Krzykacz-Hausmann, Efficient use of Monte Carlo: uncertainty propagation, Accepted for publication in Nuclear Science and Engineering (2014).

[26] P. Helgesson, D. Rochman, H. Sjöstrand, E. Alhassan, A. J. Koning, UO_2 vs MOX: propagated nuclear data uncertainty for k_{eff}, with burnup, Accepted for publication in Nuclear Science and Engineering (2013).

[27] D. Rochman, W. Zwermann, S. van der Marck, A. Koning, Uncertainty propagation with Fast Monte Carlo techniques, in: International Nuclear Data Conference for Science and Technology, New York, USA, 2013, accepted for publication.

[28] E. Alhassan, H. Sjöstrand, J. Duan, C. Gustavsson, A. Koning, S. Pomp, D. Rochman, M. Österlund, Combining Total Monte Carlo and Benchmarks for nuclear data uncertainty propagation on an LFRs safety parameters, in: International Nuclear Data Conference for Science and Technology, New York, USA, 2013, accepted for publication in Nuclear Data Sheets.

[29] H. Sjöstrand, E. Alhassan, J. Duan, C. Gustavsson, A. Koning, S. Pomp, D. Rochman, M. Österlund, Propagation of nuclear data uncertainties for ELECTRA burn-up calculations, in: International Nuclear Data Conference for Science and Technology, New York, USA, 2013, accepted for publication in Nuclear Data Sheets.

[30] J. N.Wilson, S. Siem, S. J. Rose, A. Georgen, F. Gunsing, B. Jurado, L. Bernstein, Nuclear data for reactor physics: Cross sections and level densities in the actinide region, in: EPJ Web of Conferences, Vol. 2, EDP Sciences, 2010, p. 12001.

[31] M. Johnson, S. Lucas, P. Tsvetkov, Modeling of reactor kinetics and dynamics, Laboratory IN, Idaho Falls, ID (2010) 83415.

[32] R. Meulekamp, S. van der Marck, Calculating the effective delayed neutron fraction by Monte Carlo, Nuclear Science and Engineering 152 (2) (2006) 142–148.

[33] D. E. Cullen, PREPRO 2012 ENDF/B Pre-processing Codes, IAEA report IAEA-NDS-39, 2012.
URL `https://www-nds.iaea.org/public/endf/prepro(2012)`

[34] P. Wolniewicz, C. Hellesen, A. Hakansson, S. J. Svård, P. Jansson, M. Österlund, Detecting neutron spectrum perturbations due to coolant

density changes in a small lead-cooled fast nuclear reactor, Annals of Nuclear Energy 58 (2013) 102–109.